Progress in Selective Hydrogenation: Reactivity Trends in PdAu Heterogeneous Catalysts & Developing Chiral Building Blocks for New Homogeneous Catalysts

A Senior Honors Project Presented to the Faculty of the
Department of Chemistry,
University of Hawai‘i at Mānoa

In Partial Fulfillment of the Requirements
For Bachelor of Science with Honors in
Chemistry

By Amy Chinen
14 April 2017

Committee:
Dr. Matthew Cain, Mentor
Dr. Craig Jensen

Acknowledgements

I would like to thank Dr. Raj Raman and the Center for Biorenewable Chemicals; Dr. James Dumesic, Madeline Ball, and the Dumesic Catalysis Group at the University of Wisconsin – Madison; Dr. Brant Landers, the Cain Research Group, Dr. Craig Jensen, and especially my adviser Dr. Matthew Cain and at the University of Hawai‘i at Mānoa.

Abstract

Selective hydrogenation is an essential method for converting cheap starting materials into more valuable chemical building blocks. Whether regioselectivity or diastereoselectivity is desired, catalysts are often employed to aid in this transformation. This work explores possibilities for fine-tuning both homogeneous and heterogeneous catalysts. Previously, bimetallic PdAu catalysts were used to enable the conversion of biologically produced 4-hydroxycoumarin (4HC) to pharmaceutically relevant coumarin and dihydroxycoumarin (DHC), but the subtleties of catalyst preparation and the effect of Pd loading were not known. Part I focuses on identifying reactivity trends resulting from variations in PdAu catalysts. Several PdAu catalysts with varying Pd:Au ratios were prepared by controlled surface reactions (CSR) or incipient wetness impregnation (IWI). Using high performance liquid chromatography (HPLC) and gas chromatography-mass spectrometry (GCMS), we determined the effects of the preparation method and Pd loading on reactivity, selectivity, and resistance to deactivation for the selective hydrogenation of 4HC to DHC. Part II aims to develop chiral building blocks for C_1-symmetric, P-stereogenic ligands that will be used in the asymmetric hydrogenation of heavily functionalized substrates. To date, a new diastereoselective method of adding RO-H across a P=P double bond was identified and a new sterically dominating R group was generated. The results were analyzed by nuclear magnetic resonance (NMR) spectroscopy.

Keywords: *selective hydrogenation, heterogeneous catalysis, biorenewable chemicals, asymmetric hydrogenation, homogeneous catalysis, P-stereogenic ligands*

Table of Contents

List of Figures

List of Schemes

List of Tables

PART I: Reactivity Trends in Selective Hydrogenation of 4-Hydroxycoumarin with PdAu Catalysts

Introduction

The use of fossil fuels has greatly advanced human civilization. Petroleum and petroleum-based products are employed in the production of energy, polymers, plastics, lubricants, chemicals, cosmetics, and pharmaceuticals. However, there are drawbacks to such a heavy reliance on fossil fuels. The necessary mining, drilling, and transporting of these sources has had serious negative impacts on the environment. In order to continue to advance society, it is imperative to find and implement new ways of satisfying our energy and material needs without sacrificing the environment.

Biomass is an attractive alternative to fossil fuel as it is readily available domestically, renewable, and minimally harmful to the environment. Recent research has shown that biosynthesis can be used to selectively de-functionalize biomass into useful chemicals including 4-hydroxycoumarin (4HC).[1] In the synthesis of highly oxygenated species, biomass may in fact be a more efficient source than fossil fuel.[2] Chemical catalysis offers opportunities for further upgrading these biorenewable species into fine chemicals and valuable pharmaceutical building blocks like dihydroxycoumarin (DHC).[1] Heterogeneous catalysis is favored for industrial methods due to the ease of separating the catalyst after conversion.[3]

4HC is a fused-ring system used in the synthesis of Warfarin, an anticlotting agent.[2] 4HC can be produced from plant material by polyketide biosynthesis in genetically engineered yeast, mold, and fungi.[2,4] It can be further upgraded into the valuable chemical intermediates coumarin and dihydrocoumarin (DHC) by heterogeneous chemical catalysis (Scheme 1.1).[2] Coumarin is

used in anti-inflammatory, anti-allergy, and bronchial dilation drugs, as well as cosmetics and laser dyes.[2,5] Both coumarin and DHC can be further condensed in the presence of ammonia to nitrogen-based heterocyclic compounds, the class of structures upon which many pharmaceutical and agrochemical products are constructed.[6]

Scheme 1.1. 4HC hydrogenation pathway to coumarin, DHC, and other products

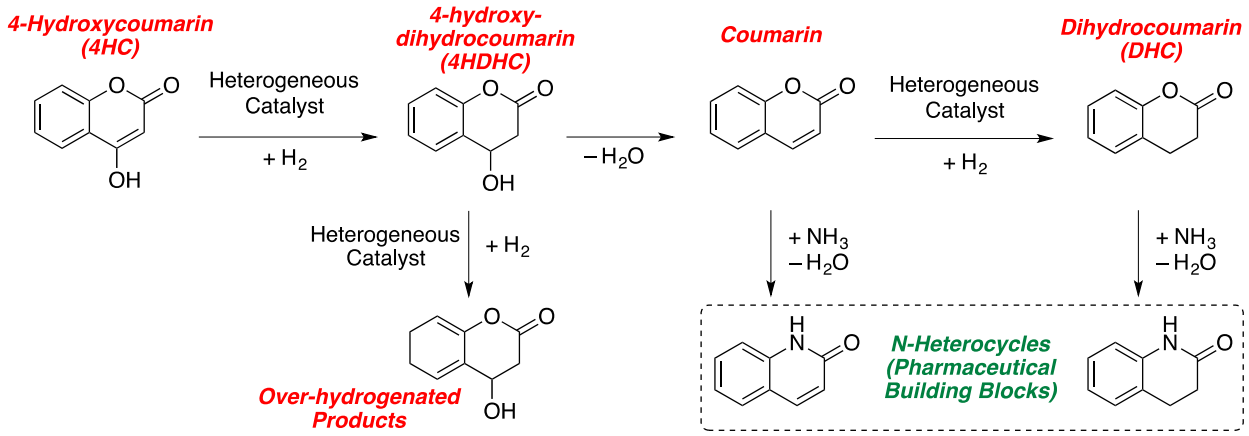

The ideal catalyst for the conversion of 4HC to DHC (Scheme 1.1) has a long lifetime and is highly active and selective for DHC. Previous work has shown supported palladium and bimetallic gold-palladium (PdAu) catalysts to be particularly effective at catalyzing this reaction.[2] Bimetallic catalysts with small, highly dispersed particles have the advantage of lowering material costs by increasing surface area for substrate adsorption. In addition to containing more active sites, metals deposited onto gold nanoparticles may have enhanced reactivity due to differences in morphology and surface electronic structure.[7] For these reasons, catalysts with palladium deposited on gold nanoparticles were selected as the focus of this work. Silica (SiO_2) was chosen as the support for its high affinity for gold and lack of interaction with palladium, and its functional inertness in the presence of 4HC. Monometallic $PdSiO_2$ catalysts were also tested and compared with bimetallic PdAu catalysts.

Part I of this thesis aims to identify trends in the effect of variations in PdAu catalysts on

the conversion of 4HC. This will positively impact society by increasing the feasibility of upgrading biosynthetically produced chemicals into fine chemicals and pharmaceuticals, thereby reducing reliance on fossil fuels.

Research Objectives

1. Identify trends in conversion for monometallic and bimetallic catalysts with varying Pd loads at the same time scale in hydrogenation of 4HC to DHC

2. Identify trends in selectivity for monometallic and bimetallic catalysts with varying Pd loads at the same conversion in hydrogenation of 4HC to DHC

3. Determine deactivation rate of catalysts in hydrogenation of 4HC to DHC

Scheme 1.2. 4HC hydrogenation pathway to coumarin and DHC

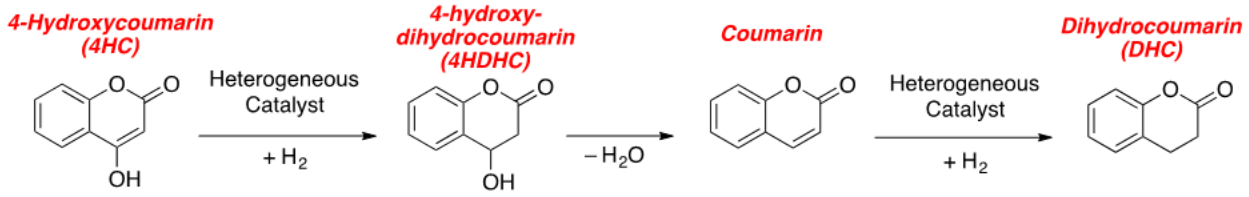

Methodology

Synthesis of Monometallic Catalyst

A monometallic Pd/SiO_2 catalyst with 2 wt% Pd load on silica support was prepared by incipient wetness impregnation (IWI). Prior to impregnation, the silica was acid washed by treatment with 750 mL of deionized water and 5 mL of 0.1 M solution of HNO_3 (aq) at room temperature for 1 h. The mixture was filtered and dried in air at 100 °C. An aqueous solution of $Pd(NO_3)_2$ (10 wt% Pd, 0.879 g, 5.22 mmol) was then added dropwise to the silica under manual stirring. The Pd-impregnated support was dried in an oven at 383 K overnight. The resulting solid was reduced under H_2 at 773 K for 45 min then passivated with 1% O_2 in Ar for 0.5 h at room temperature to afford the catalyst.

Synthesis of Bimetallic Catalysts

Several AuPd bimetallic catalysts with Pd loading ranging from 0.07 to 0.87 wt% (as determined by ICP) on silica support were synthesized. To deposit small, highly dispersed gold nanoparticles on the support material, monometallic Au/SiO_2 was first produced by deposition precipitation in the manner described by Li.[8] Acid washed silica (5 g) was added to ~200 mL deionized water and stirred for 0.5 h at room temperature. Meanwhile a solution of 0.2 M $HAuCl_4$ was prepared by treatment of an aqueous solution of $HAuCl_4$ aqueous solution (0.604 g, 1.78 mmol $HAuCl_4$) with 9 mL deionized water and added to the silica slurry. A 0.1 M solution of NaOH was added to the suspension to achieve pH 9 and the mixture was stirred for 6 h, keeping the pH constant. The mixture was then filtered and washed with deionized water. The resulting solid was dried in air at 383 K overnight and then reduced in flowing H_2 at 623 K. Pd was then deposited onto the gold by controlled surface reactions (CSR) as delineated by C. Sener.[9] Briefly, the

Au/SiO_2 produced by deposition precipitation was reduced in a Schlenk tube under H_2 at 623 K, sealed, and placed in a glove box under Ar. Also in the glove box, Pd was suspended in *n*-pentane to give the desired loading. The Schlenk tube was unsealed, and the Pd solution added. This mixture was stirred for 1 h. The Schlenk tube was removed from the glove box and remaining solvent was evaporated under vacuum. The sample was reduced under H_2 at 773 K for 45 min then passivated with 1% O_2 in Ar for 0.5 h at room temperature to afford the catalyst.

Characterization of Catalysts

Catalysts were analyzed to determine wt% Au, wt% Pd, Au:Pd, average particle size, and dispersion. Weight percents (wt%) of Au and Pd were determined by inductively-coupled plasma mass spectrometry (Perkin-Elmer 400 ICP Emission Spectrometer). Particle size and distribution of PdAu catalysts were determined by transmission electron microscope (FEI Titan STEM with Cs probe aberration corrector at 200 kV with spatial resolution < 0.1 nm) and energy dispersive X-ray spectroscopy (EDS).

Reaction Method

The reaction method for hydrogenation of 4HC to DHC was based on the work of Schwartz.[2] The catalyst, a magnetic stir bar, and feed solution were loaded into a Hastelloy pressure vessels (Parr Instruments, Model 3010). The feed consisted of 2 wt% 4HC dissolved in tetrahydrofuran (THF). The vessel was sealed and purged with argon, then pressurized to 30 bar (30 atm) with H_2. The reactions were carried out at 348 K under 30 bar of H_2 and stirred at 500 rpm in a multireactor stirrer system (Parr Instruments, Model 5000).

I. Conversion

Each catalyst was subjected to the above reaction method for 6 h. The products of each reaction (4HDHC, coumarin, DHC, and overhydrogenated products) were compared and analyzed by high performance liquid chromatography (HPLC) to evaluate any trends in conversion. (See Analysis section below.) Trends based on Pd loading and differences in conversion between monometallic and bimetallic catalysts were of particular interest.

II. Selectivity

Once a relationship was identified between Pd loading, duration of reaction, and conversion, the resulting curve was used to calculate the catalyst to feed ratio and reaction duration required to bring reactions to 5% conversion using each of the catalysts in order to assess the selectivity at the early stage. The products at 5% conversion were analyzed by HPLC to determine the differences in selectivity between monometallic and bimetallic catalysts.

III. Deactivation

A final aspect of the catalytic reaction we wanted to explore was deactivation. Each catalyst was deployed in the standard reaction method for a duration of four hours. Following this reaction, a sample of the resulting solution was taken for HPLC to determine conversion and selectivity. The remaining solution was filtered, washed with THF, and dried overnight in a 313 K oven. The reaction was then repeated with an equal catalyst to feed ratio for the amount of recovered catalyst. This process was repeated until three reactions had been carried out with the same catalyst.

Analysis of Reaction Results

The primary method of analysis was reverse-phase HPLC (Waters Alliance 2695 system

with Waters 996 UV detector and reverse-phase Agilent Zorbax SB-C18 column (4.6mm × 300 mm, 5 μm), using 5 mM H_2SO_4 as the aqueous phase and acetonitrile as the organic modifier). Samples of feed and postreaction fluid were filtered through 0.22 μm syringe filters before injection. All samples were taken in triplicate, and the results averaged to give a robust value with associated standard deviation. In order to identify the peaks and determine product concentration, standards of known identity and concentration were produced and injected in the HPLC to produce calibration curves.

The identities of the products were verified using HPLC fraction collection and gas chromatography/mass spectrometry (Shimadzu GCMS-QP2010 with flame ionization detector (FID) and DB-5MS capillary column). As products (fractions) eluted from the HPLC column they were collected in test tubes. Samples of each fraction were then analyzed by GC/MS and the spectra compared against the NIST Standard Reference Database 1A v14.

Results & Discussion

Catalysts

Five bimetallic PdAu catalysts were synthesized by deposition precipitation followed by CSR. The Au:Pd ratios were determined by EDS and wt% Pd by ICP. The results are presented in Table 1.1. One monometallic Pd/SiO_2 catalyst was also synthesized with 2 wt% Pd.

Table 1.1. Analysis of PdAu catalysts

Catalyst #	Theoretical Au:Pd	EDS Au:Pd	ICP wt% Pd
15	1:0.15	1:0.15	0.24
16	1:0.06	1:0.18	0.07
17	1:0.30	1:0.13	0.39
19	1:0.30	1:0.07	0.54
20	1:0.45	1:0.21	0.87

TEM images confirmed that small, highly dispersed particles were produced (Figures 1.1 and 1.2).

Figure 1.1. TEM image of Catalyst #15

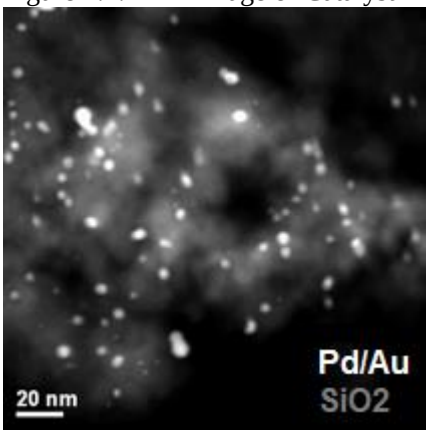

Figure 2.1. TEM image of catalyst #16

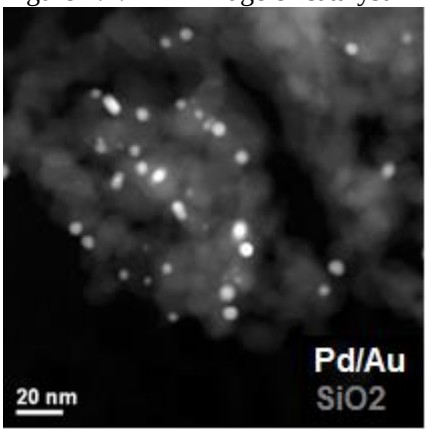

Conversion

Reaction Method I was used to investigate the overall conversion of 4HC to 4HDHC, coumarin, and DHC by each of the six catalysts on the same timescale (Table 1.2). Conversion percentage was determined by HPLC and product identities were confirmed by GC/MS.

Table 1.2. Pd loading and conversion from 4HC

Entry	**Catalyst #**	**Material**	**wt% Pd**	**% Conversion**
1	16	$PdAu/SiO_2$	0.07	0.20
2	15	$PdAu/SiO_2$	0.24	2.50
3	17	$PdAu/SiO_2$	0.39	4.73
4	19	$PdAu/SiO_2$	0.54	9.70
5	20	$PdAu/SiO_2$	0.87	17.90
6	99	Pd/SiO_2	2.0	5.0

A clear trend can be identified between Pd loading and % conversion. In the case of PdAu catalysts, increasing the Pd loading increased conversion for all catalysts. The monometallic catalyst (Entry 6) had the highest wt% Pd, but its overall conversion was similar to that of the PdAu catalyst with one-fifth the Pd loading (Entry 3). This suggests that bimetallic PdAu catalysts of higher Pd loading led to increased activity. Figure 1.3 illustrates the trend.

Figure 1.3. Pd loading and conversion chart

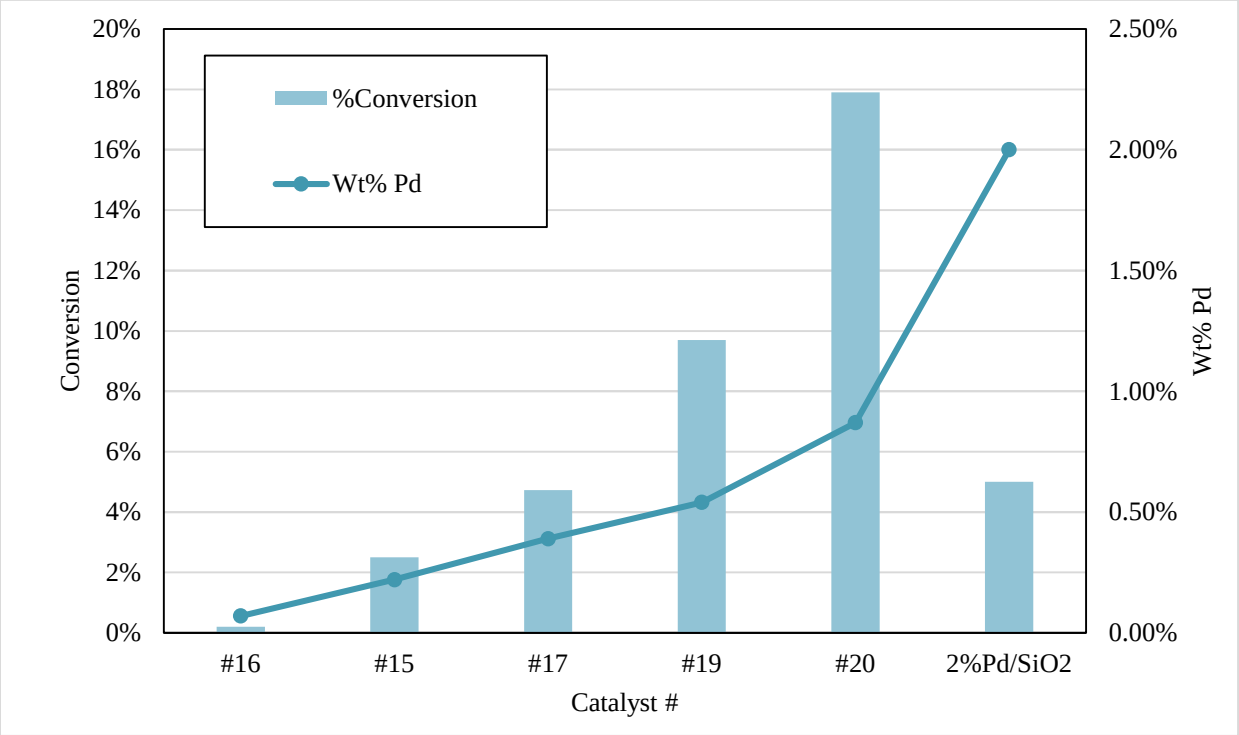

Selectivity

Reaction Method II was used to determine the selectivity of the catalysts at the same percent conversion. Four catalytic reactions were halted at the target conversion of approximately five percent and their selectivity was analyzed by HPLC. The results are summarized in Table 1.3.

Table 1.3. Selectivity at similar conversion

Catalyst #	wt% Pd	% Conversion	4HDHC	coumarin	DHC	over-hydrogenated
17	0.39	4.7	53.2	2.0	44.2	0.6
19	0.54	5.5	59.6	3.0	34.9	2.5
20	0.87	5.6	59.3	0.7	37.8	2.2
99	2.0	5.0	64.7	0.4	31.3	3.6

Among the catalysts tested, there is a similar distribution of products at the same conversion. A slight trend emerges that higher Pd loading increases overhydrogenated products and 4HDHC and decreases DHC and coumarin (Figure 1.4).

Figure 1.4. Selectivity at 5% conversion

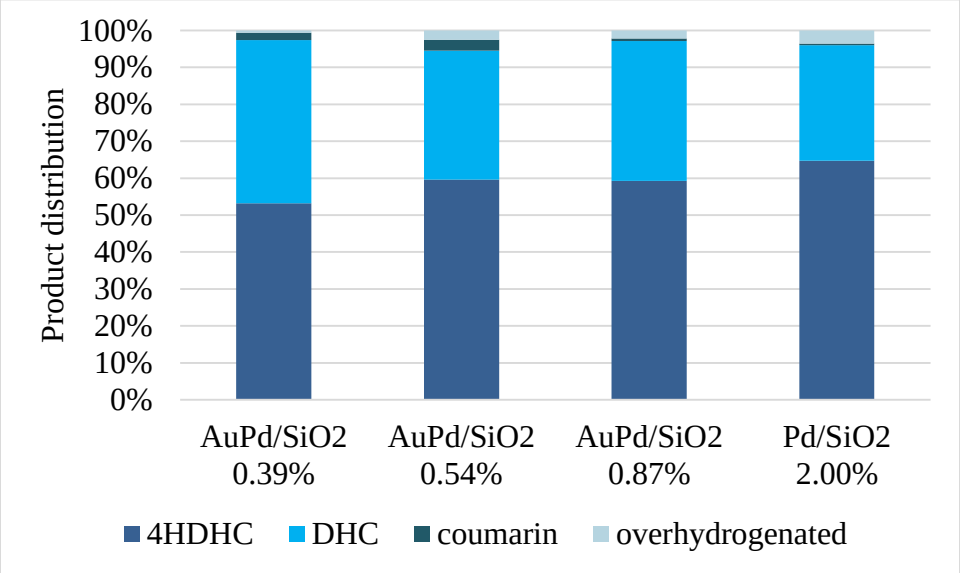

A closer look at the distribution of the minor products, coumarin and overhydrogenated products, shows an effect on the catalysts' selectivity for these products that may be associated with Pd loading (Figure 5). As Pd loading increased, overhydrogenation also generally increased,

and selectivity for coumarin decreased.

Figure 1.5. Coumarin and overhydrogenated product selectivity

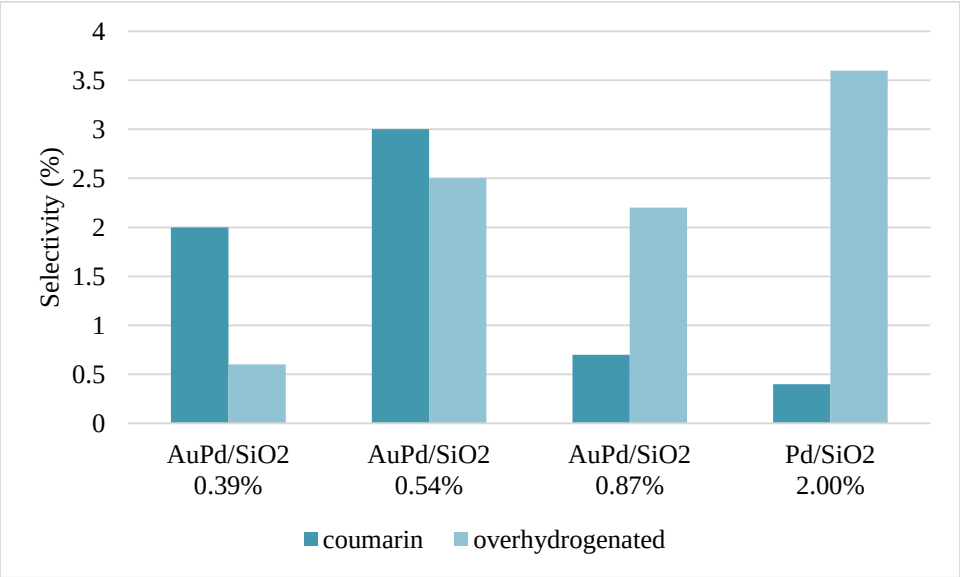

Deactivation

Reaction Method III was used to investigate the rate and degree to which two catalysts, #19 ($PdAu/SiO_2$) and #99 (Pd/SiO_2), deactivated with continued use over time. These catalysts were selected for the purpose of comparing the deactivation of monometallic and bimetallic catalysts.

The results were mixed (Figure 1.6). Both catalysts decreased in effectiveness after the first cycle, but the results show increased conversion in the third cycle. In the case of the monometallic Pd catalyst, conversion in the third cycle actually appears higher than in the first cycle. This may be the result of error or decomposition into an unidentified catalyst species, potentially nanoparticles. However from these results we can infer that some deactivation does occur with use in both catalysts, and that neither deactivates completely after three four-hour reaction cycles.

Figure 1.6. Deactivation of catalysts over three reaction cycles

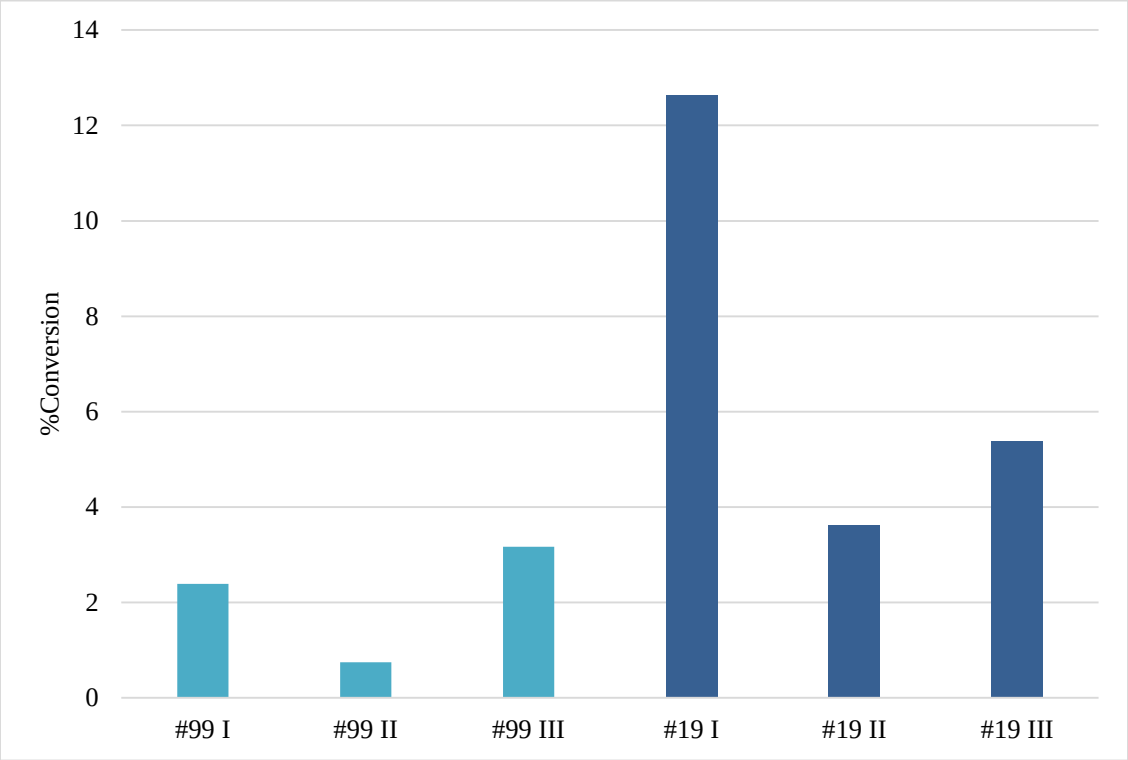

Conclusions & Future Work

This study has identified trends in the palladium-catalyzed hydrogenation of 4HC based on the composition of the heterogeneous catalyst. Bimetallic $PdAu/SiO_2$ catalysts with Pd loading ranging from 0.07 to 0.87% were investigated, and catalysts with high loadings demonstrated increased conversion of 4HC to its hydrogenated products. There is likely an upper limit to the amount of Pd that can be deposited on the catalyst before the active sites become crowded and conversion diminishes with increasing Pd loading due to dendritic effects.[10] Further research is needed to determine this limit. The number of active sites may also be determined by chemisorption, which would give more insight into the relationship between Pd loading and catalytic activity than merely comparing wt% Pd as was done in this study. It is important to optimize the loading to balance cost and effectiveness.

The bimetallic $PdAu/SiO_2$ catalysts significantly outperformed the monometallic Pd catalyst in overall conversion. The addition of gold to the catalyst led to a factor of five increase in conversion versus Pd/SiO_2. This is important because catalytic materials are expensive, so increasing their effectiveness means reducing the cost of these reactions and increasing feasibility.

At 5% conversion, some selectivity trends were observed. Higher Pd loadings increased 4HDHC and overhydrogenation and decreased DHC and coumarin products. This trend included the monometallic and bimetallic catalysts without distinction. Overhydrogenated products are undesirable because retaining the aromatic ring is necessary for the target products. It will be important in an industrial setting to balance the benefit of increased overall conversion with high Pd loading with the concomitant effect of higher undesired products.

Finally, it was difficult to gauge the rate and degree of catalyst deactivation in the batch

reactor. Activity appeared to decrease in the second cycle then increase in the third; an unlikely scenario. It is possible that the catalyst was not rinsed well enough between the second and third cycles and some product was transferred to the subsequent experiment, skewing the results. Coperét has also attributed increased activity over multiple cycles to breakdown of catalysts into nanoparticles, increasing surface area.[11] A better way to investigate the cause and extent of deactivation would be with a flow reactor.

PART II: Developing Chiral Building Blocks for C_1-Symmetric, P-stereogenic Ligands

Introduction

The discovery of teratogenic effects resulting from one enantiomer of the sedative thalidomide in the early 1960s demonstrated the importance of enantioselective synthesis in pharmaceutical production. Launched as the racemate in 1957, thalidomide was withdrawn from the market in 1961 when its use had caused malformation in more than 10,000 children born to mothers who used the drug in the first trimester of pregnancy.[1] It was discovered that one enantiomer had the desired therapeutic effect, while the other caused fetal abnormalities.

Asymmetric hydrogenation is an important method of generating stereogenic centers in pharmaceuticals.[2] At present, most asymmetric reactions in the pharmaceutical industry utilize a combination of alkenes, which are activated or feature directing groups and privileged C_2-symmetric scaffolds such as BINAP, DuPhos, and DiPAMP (Figure 2.1).[3] Despite this success, a major gap exists in the design of new ligands and catalysts capable of hydrogenating more densely substituted "problem substrates," such as α,β unsaturated nitriles, substituted quinolines, imines, and highly substituted olefins.[4]

Figure 2.1. Typical substrates, ligands, and binding pocket

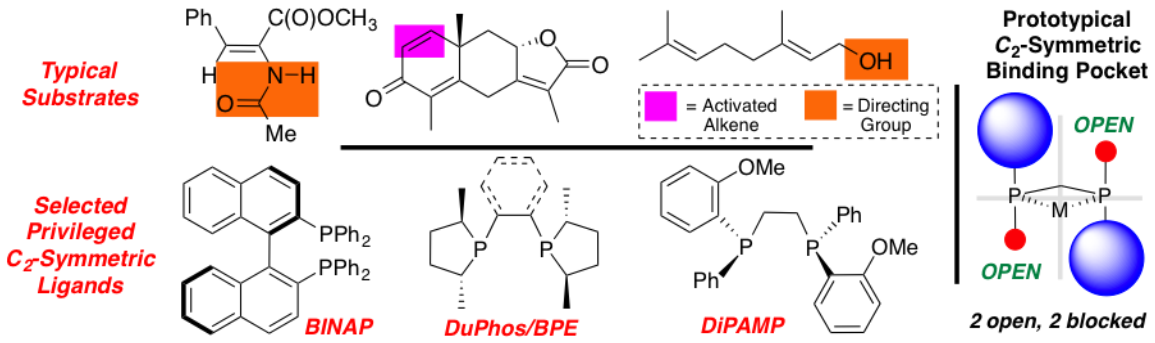

The Cain group has hypothesized that C_1-symmetric, P-stereogenic ligands constructed from prochiral phosphaalkenes may remedy this issue and enable highly selective asymmetric hydrogenation of "problem substrates".[5,6] These ligands feature sterically dominating P-stereocenters to maximize enantioselectivity and a modular and tunable second donor group to customize the binding pocket from severely sterically crowded to largely open (Figure 2.2). These features permit the optimization of the asymmetric environment for each substrate tested.

Figure 2.2. Tunable binding pocket

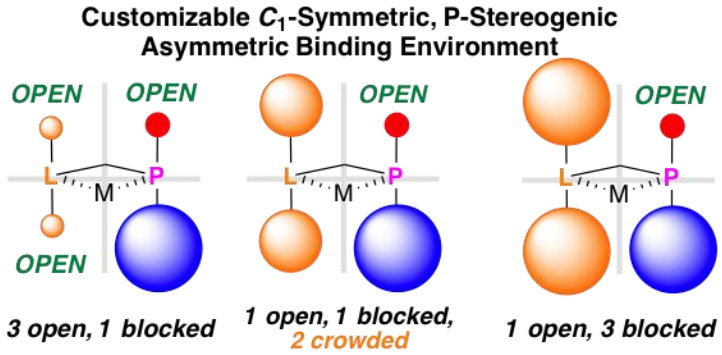

There are two approaches to constructing the target ligands: 1) chiral building block to chiral ligand, and 2) prochiral phosphaalkenes ligand to chiral ligand (Scheme 2.1).

Scheme 2.1. Two approaches to C_1-symmetric, P-chiral ligands

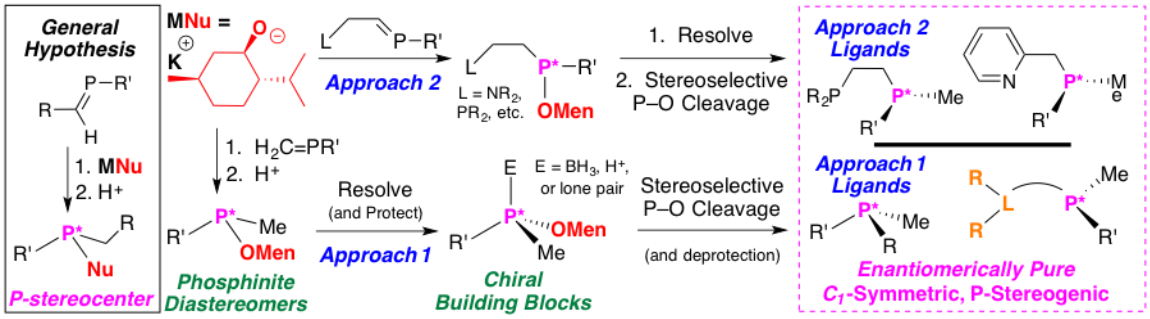

To construct chiral phosphine ligands via Approach 1, the phosphaalkene lone pair is coordinated with a simple Lewis acid such as K^+, promoting nucleophilic attack at phosphorus and

generating a stereocenter.[7] Utilizing the mentholate anion as the nucleophile results in phosphinite diastereomers; resolution followed by stereoselective P-O bond cleavage affords enantiomerically pure C_1-symmetric, P-stereogenic ligands (Scheme 2.1, top).[8] The second approach involves converting pre-constructed phosphaalkene-derived multidentate ligands into P-stereogenic compounds via chiral alcohol addition (Scheme 2.1, bottom).[9]

Research Objective

Develop chiral building blocks and prochiral phosphaalkene ligands for use in C_1-symmetric, P-stereogenic ligands

Methodology

Reactions were conducted using anhydrous solvents under an inert atmosphere of nitrogen unless otherwise stated. Thin-layer chromatography (TLC) was performed using Sigma-Aldrich silica gel precoated glass plates and visualized under ultraviolet light (254 nm). Column chromatography was carried out using Fischer 230-400 mesh silica gel. ^{1}H and $^{31}P\{^{1}H\}$ NMR spectra were recorded using an Agilent DD2 spectrometer at 300 MHz. ^{1}H NMR chemical shifts are reported relative to $CDCl_3$ signals and data is reported as follows: chemical shift (δ ppm), multiplicity, coupling constant (Hz), and integration. All chemicals were used as received except **1** and **4** which were synthesized by Dr. Brant Landers.

Product **3**

Scheme 2.2. Synthetic pathway to **3**

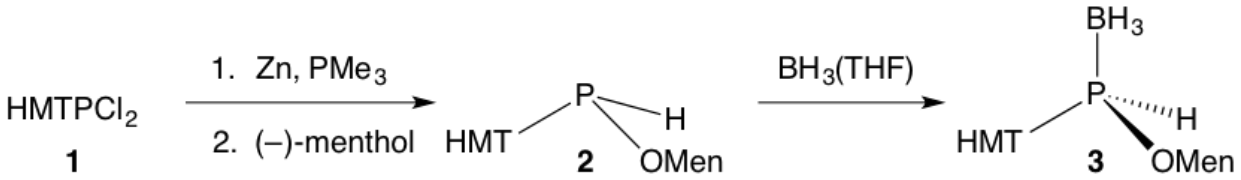

In a dry glove box under an inert atmosphere of N_2, a suspension of zinc dust (0.05 g, 0.001 mmol, 1.0 equiv) and $HMTPCl_2$ (0.33 g, 0.001 mmol, 1.0 equiv) in 5 mL of benzene was treated with PMe_3 (0.15 g, 0.002 mmol, 2.5 equiv) and stirred for 1 h. In a separate vial, a solution of (-)-menthol (0.15 g, 0.001 mmol, 1.2 equiv) in 5 mL of benzene was transferred to a Schlenk flask fitted with a fritted filter and the $HMTPCl_2$ mixture was filtered under vacuum into the homogeneous solution. The filter and vial were rinsed with benzene (5 mL) and the Schlenk flask sealed. The mixture was stirred for 24 h to afford crude product **2** as an oil (dr = 70:30): ^{31}P NMR (121 MHz, $CDCl_3$) δ 80.80 (dd, J = 199, 13 Hz), 73.09 (dd, J = 195, 10 Hz) The mixture containing **2** was filtered under nitrogen into a second Schlenk flask and the flask and filter rinsed with THF

(5 mL). The solution was concentrated under vacuum and the resulting solid dissolved in THF (5 mL). The flask was removed from the glove box. In a fume hood, BH_3 in THF (1.0 M, 4.7 mL, 0.005 mmol, 6 equiv) was added dropwise via syringe to the flask and the resulting solution stirred 1 h. The reaction was quenched with H_2O. The solution was transferred to a separatory funnel and the aqueous layer extracted with DCM (3 × 10 mL). The combined organic layers were dried over $MgSO_4$, filtered through Celite, and the filtrate was concentrated under vacuum affording a crude solid. Thin layer chromatography (TLC) analysis (90:10 hexanes/EtOAc) indicated the presence of both diastereomers of product **3** (dr = 65:35): ^{31}P NMR (121 MHz, $CDCl_3$) δ 86.7 (br), 77.6 (br).

Product **6**

Scheme 2.3. Synthetic pathway to **6**

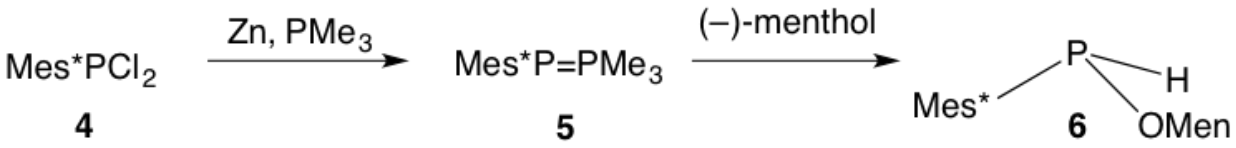

4 **5** **6**

In a glove box under N_2, zinc dust (0.02g, 0.29 mmol, 1.0 equiv) and THF (2 mL) was added to a vial containing **4** (0.10 g, 0.29 mmol, 1.0 equiv) and treated with PMe_3 (0.05 g, 0.72 mmol, 2.5 equiv) in benzene and stirred for 1 h. The resulting mixture was transferred to a Schlenk flask and (-)-menthol (0.09 g, 0.58 mmol, 1.2 equiv) was added. The flask was removed from the glove box and stirred for 4 h in a fume hood. The solution was concentrated under vacuum to afford product **6**. ^{31}P NMR (121 MHz, $CDCl_3$) δ 71.06 (dd, J^1_{PH} = 210.6, 7.9 Hz), 67.43 (dd, J = 67, 9 Hz).

Phospha-Wittig reaction to product **10**

Scheme 2.4. Phospha-Wittig reaction

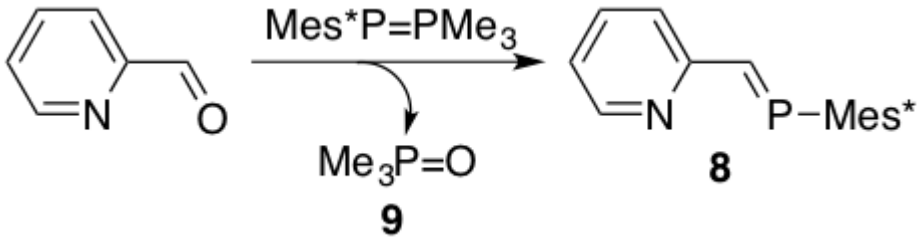

In a glove box under N_2, a mixture of **4** (2.0 g, 5.76 mmol, 1.0 equiv) and zinc dust (1.0 g, 5.76 mmol, 1.0 equiv) was treated with a solution of PMe_3 (1.1 g, 14.40 mmol, 2.5 equiv) in 2 mL THF for 1 h. 2-Pyridinecarboxaldehyde (0.6 g, 5.47 mmol, 0.95 equiv) was added, the flask was sealed under N_2 and stirred for 4 h in a fume hood. The solution was concentrated under vacuum to yield a mixture of **8** and **9** and returned to the glove box. The mixture of **8** and **9** was dissolved in pentane and filtered through Celite to remove **9**. The resulting solution was concentrated under vacuum to yield purified product **8 (**1.1 g, 2.99 mmol, 55% yield). ^{31}P NMR (121 MHz, THF): δ 284.

Scheme 2.5. (*R*)-BINOL addition to phospha-Wittig product

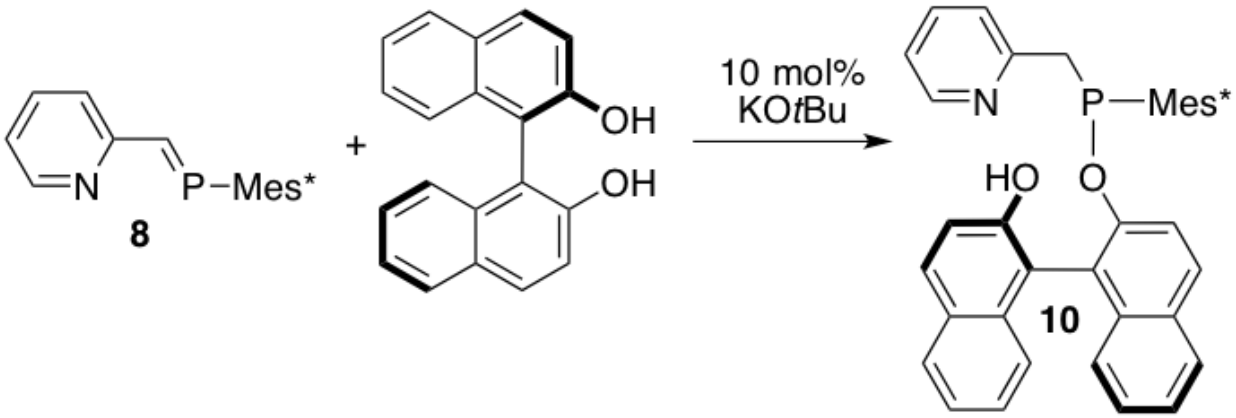

Pyridine-phosphaalkene **8** (1.1 g, 2.99 mmol, 1.0 equiv) was transferred to a Schlenk bomb

and (*R*)-BINOL (0.9 g, 3.29 mmol, 1.1 equiv) was added. The mixture was dissolved in DCM (20 mL) & potassium tert-butoxide (KOtBu) (0.03 g, 0.30 mmol, 10 mol%) was added. The Schlenk bomb was sealed and removed from the glove box to an ice bath in a fume hood. The reaction mixture was stirred for 6 h then concentrated under vacuum to afford **10** as a solid (dr = 2:1): ^{31}P NMR (121 MHz, THF): δ 118, 116. ^{1}H NMR spectrum was also recorded but was difficult to interpret due to the presence of both diastereomers and overlap of the aryl regions.

(2,4,6-Tricyclohexylphenyl)phosphonous dichloride **13**

Scheme 2.6. Alkylation and bromination of benzene, substitution to **13**

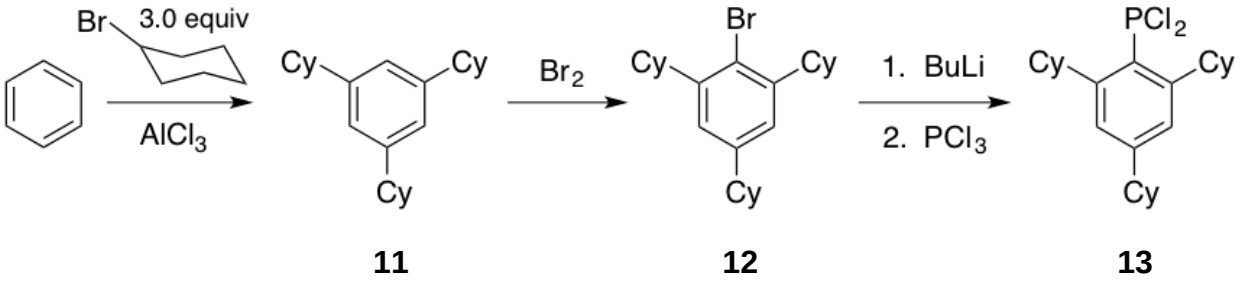

11 **12** **13**

In a fume hood under N_2, a three-necked round bottom flask containing a magnetic stir bar and $AlCl_3$ (38 g, 285 mmol) was placed in an ice bath. Benzene (8 mL) and DCM (60 mL) were added dropwise via dropping funnel while stirring. Cyclohexyl bromide (35 mL, 487 mmol, 3.0 equiv) was added via syringe to the dropping funnel and added dropwise to the flask and the resulting mixture stirred for 2 h. The reaction was quenched slowly with ice (50 mL), and ether (200 mL) was added. The mixture was transferred to a separatory funnel and washed with water (2 × 50 mL) and brine (50 mL). The organic layer was dried over $MgSO_4$, filtered, and the filtrate was concentrated under vacuum. The product was purified by column chromatography in silica gel with hexane as the solvent. The first fraction was collected and concentrated under vacuum to afford **11** (24.36 g, 75.06 mmol, 46% yield). The flask containing **11** was transferred to a glove

box and dissolved in 15 mL of $CHCl_3$. Br_2 (3.6 mL, 70.2 mmol, 1.0 equiv) was added at 0°C over the course of 15 min via a dropping funnel. The funnel was rinsed with $CHCl_3$ (5 mL) and the rinse was added to the flask. The flask was removed from the ice bath and stirred 2 h, venting periodically with N_2. The resulting solution was diluted with DCM (50 mL) and washed with H_2O (100 mL). The mixture was transferred to a separatory funnel, the aqueous layer extracted with DCM (3 × 50 mL), and the combined organic layers were washed with NaOH (10 wt%, 50 mL) and brine (50 mL). The organic fraction was dried over $MgSO_4$ and filtered into a round-bottom flask and concentrated under vacuum. The product was purified by column chromatography in silica gel with hexane and then DCM as the eluents. The first fraction was collected and concentrated under vacuum until dry. The resulting solid was titrated with EtOAc and stirred for 20 min. The solution was filtered and washed with EtOAc (25 mL) then dried under vacuum to give product **12** (12.433 g, 30.8 mmol, 44% yield): ^{1}H NMR (C_6D_6): δ 1.35 (s, 9H), 1.58 (s, 18H), 7.42 (s, 2H) The following procedure was adapted from a method developed by Cowley.[10] A solution of **12** (12.433 g, 30.8 mmol, 1.0 equiv) in THF (120 mL) was placed in a Schlenk flask, cooled to -78°C, and treated with BuLi in hexanes (1.6 M, 21.2 mL, 33.9 mmol, 1.1 equiv) and the mixture was stirred for 2 h at -78°C to generate the lithiated product as an oil. PCl_3 (2.9 mL, 33.9 mmol, 1.1 equiv) was placed in a second Schlenk flask cooled to -78°C. The solution containing the lithiated product was transferred quantitatively via cannula into the second flask over 30 min, maintaining both flasks at -78°C. The product mixture was warmed to room temperature and stirred for 2h, then concentrated under vacuum and transferred to the glove box. Pentane (5 mL) was added and the resulting mixture was filtered through Celite into a filter flask and rinsed with more pentane (5 mL). The resulting solid was dissolved in ether (5 mL) and filtered again. The solution was concentrated under vacuum to afford the crude product **13**. ^{1}H NMR (300 MHz,

$CDCl_3$) δ 7.08 (d, *J* = 3.4 Hz, 2H), 2.5 (m, 2 H), 2.09-1.72 (m, 8H), 1.61-1.20 (m, 18H)

Results & Discussion

A simple two-step procedure (Scheme 2.2) involving the reduction of $HMTPCl_2$ with zinc dust, followed by treating with PMe_3 and exposure to (-)-menthol with protection from BH_3 produced **3**. Once resolved, this product will be a useful building block to new chiral phosphine ligands. This HMT derivative represents an alternative pathway to chiral building blocks, which may not be isolable or resolvable via the traditional Mes* route.

Secondary phosphinite **6** was also accessed via related chemistry. However, initial investigations by Dr. Landers into the feasibility of a second approach using (-)-menthol as the chiral group yielded an oily product which did not effectively recrystallize. We attempted to solve this problem by using (*R*)-BINOL as the chiral element in the synthesis of **10**. (*R*)-BINOL features axial chirality and possible use as a pincer ligand when incorporated into the pyridine-phosphaalkene scaffold. Synthesis and purification of **8** from **9** (Scheme 2.4) was accomplished in 55% yield. Diastereoselective addition of (*R*)-BINOL (Scheme 2.5) afforded **10** with a dr of 2:1. Resolution efforts are ongoing.

<u>New Phosphaalkene R Groups</u>

Initial investigations indicated a limitation in the phospha-Wittig approach if the R group in $RP{=}PMe_3$ is not sufficiently large ($R \geq$ Mes*, Mes* = 2,4,6-tri-*tert*-butylphenyl).[11] Coordination of smaller R groups led to oligomerization of target molecules. We were curious if new sterically-demanding P-R substituents could be developed.

Figure 2.3. Sterically bulky R groups

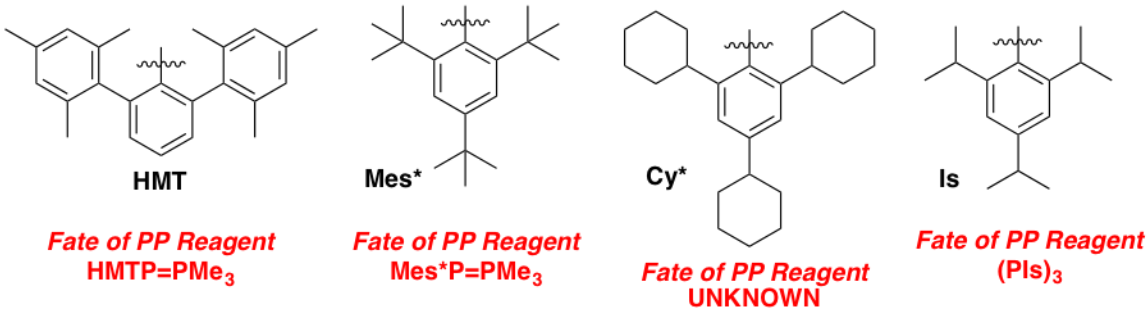

Synthesis of **13** (Scheme 2.6) was undertaken to investigate whether an additional group, tricyclohexylbenzene was sufficiently bulky to prevent undesirable oligomerization. It was hoped that a solid product could be obtained and the product purified by recrystallization; however, the product was oily and separation was not achieved despite several attempts.

Conclusions and Future Work

This study has identified pathways to synthesizing chiral building blocks for C_1-symmetric, P-stereogenic ligands. A method to resolve the diastereomers of **3** will be needed to access the desired ligands. A later iteration of this synthesis method by Dr. Landers found that addition of HCl (1 equiv) in the initial step improved the result. Addition of a base to phosphine-borane **3** will deprotonate the PH unit yielding an anion which will readily accept an R group (like Mes*), followed by removal of the BH_3 protecting group and finally coordination to a metal center. This approach is expected to afford highly customizable catalysts with a tunable binding pocket for asymmetric hydrogenation of problem substrates. Product **6** shows similar promise. A variety of building blocks is needed to afford the customizability necessary to build catalysts capable of selectively hydrogenating specific substrates.

Synthesis of product **10** demonstrates that (*R*)-BINOL can replace (-)-menthol in diastereoselectively generating a P-stereocenter. The diastereomers need to be resolved by recrystallization or chromatography. Addition of an acid such as HCl will protonate the sp^2 nitrogen or complexation of the phosphorous center with a soft acid such as Ag(I) or Cu(I) and may enhance crystallinity or separation.[12] Stereoselective P-O cleavage is expected to afford a C_1-symmetric, P-stereogenic ligand via Approach 2.

Failure to achieve recrystallization in product **13** illustrates the importance of sufficient steric bulk in the selection of R groups to afford stability of the substituent by preventing oligomerization. In this regard, Mes* is generally successful and HMT occasionally works. These groups contain outer isopropyl and methyl substituents, respectively. This work has shown that addition of PCl_2 to tricyclohexylbenzene produces the desired molecule without oligomerization,

but results in an oily product which we were not able to purify. It may still be possible to recrystallize **13** through the use of other solvents or another method. Addition of methyl or isopropyl substituents to the cyclohexyl rings would add steric bulk and may give a result more like the successful groups Mes* and HMT. More research is also needed to identify other possible sterically bulky R groups that will allow for both customizability and crystallinity in chiral ligand building blocks.

References

PART I

1. Schwartz, T. J.; Shanks, B. H.; Dumesic, J. A. *Curr. Opin. Biotech*. **2016**, 38, 54-62.

2. Schwartz, T. J.; Lyman, S. D.; Motagamwala, A. H.; Mellmer, M. A.; Dumesic, J. A. *ACS Catal*. **2016**, 6, 2047-2054.

3. Nørskov, J. K.; Studt, F.; Abild-Pedersen, F.; Bligaard, T. *Fundamental Concepts in Heterogeneous Catalysis*. John Wiley & Sons: New York, 2014.

4. Liu, B.; Raeth, T.; Beurle, T.; Beerhues, *L. Plant Mol. Biol*. **2010**, 72, 17-25.

5. Gasparetto, J.C.; Guimaraes de Francisco, T.M; Campos, F.R.; Pontarolo, R. *J. Sep. Sci.* **2011**, 34, 740–748.

6. Sridharan, V.; Suryavanshi, P.A.; Menendez, J.C. *Chem. Rev.* **2011**, 111, 7157-7259.

7. Zhang, G.-R.; Zhao, D.; Feng, Y.-Y.; Zhang, B.; Su, D. S.; Liu, G.; Xu, B.-Q. *ACS Nano*. **2012**, 6(3), 2226-2236.

8. Li. Li, W.-C.; Comotti, M.; Schüth, F. *J Catal.* **2006**, 237, 190-196.

9. Sener, C.; Wesley, T. S.; Alba-Rubio, A. C.; Kumbhalkar, M. D.; Hakim, S. H.; Ribeiro, F. H.; Miller, J.T.; Dumesic, J.A. *ACS Catal*. **2016**, 6, 1334-1344.

10. Tomalia. D. *New J. Chem*. **2012**, 36, 264-281.

11. Tada, S.; Thiel, I.; Lo, H.-K.; Copéret, C. *Chimia*, **2015**, 69(12), 759-765.

PART II

1. Eriksson, T.; Björkman, S.; Höglund, P. *Eur. J. Clin. Pharmacol*. **2001**, 57, 365-376.

2. Knowles, W.S.; Noyori, R. *Acc. Chem. Res*. **2007**, 40, 1238-1239.

3. Lennon, I.C.; Pilkington, C.J. *Synthesis.* **2003**, 11, 1639-1642.

4. Traverse, J.F.; Snapper, M.L. *Drug Discovery Today* **2002**, 7, 1002-1012.

5. Magnuson, K.W.; Oshiro, S.M.; Gurr, J.R.; Yoshida, W.Y.; Gembicky, M.; Rheingold, A.L.; Hughes, R.P.; Cain, M.F. *Organometallics* **2016**, 35, 855-859.

6. Miura-Akagi, P.M.; Nakashige, M.L.; Maile, C.K.; Oshiro, S.M.; Gurr, J.R.; Yoshida, W.Y.; Royappa, A.T.; Krause, C.E.; Rheingold, A.L.; Hughes, R.P.; Cain, M.F. *Organometallics* **2016**, 35, 2224-2231.

7. Mathey, F. *Acc. Chem. Res.* **1992**, 25, 90-96.

8. Dutartre, M.; Bayardon, J.; Jugé, S. *Chem. Soc. Rev.* **2016**, 45, 5771-5794.

9. van der Sluis, M.; Beverwijk, V.; Termaten, A.; Gavrilova, E.; Bickelhaupt, F.; Kooijman, H.; Veldman, N.; Spek, A.L. *Organometallics* **1997**, 16, 1144-1152.

10. Cowley, A. H.; Norman, N. C.; Pakulski, M. *Inorg. Synth.* **1990**, 27, 235-240.

11. Shah, S.; Protasiewicz, J.D. *Chem. Commun.* **1998**, 1585-1586.

12. Liu, X.; Braunstein, P. *Inorg. Chem.* **2013**, *52*, 7367-7379.